

A Novel Octapeptide Derived From G Protein-Coupled Receptor 124 Improves Cognitive Function Via Pro-Angiogenesis In A Rat Model Of Chronic Cerebral Hypoperfusion-Induced Vascular Dementia

This article was published in the following Dove Press journal:
Drug Design, Development and Therapy

Ying Xiao¹
Hong Shen²
Rui Li³
Xia Zhou²
Hong Xiao²
Jun Yan⁴

¹College of Science, China Pharmaceutical University, Nanjing, People's Republic of China; ²Neuro-Psychiatric Institute, Nanjing Medical University Affiliated Brain Hospital, Nanjing, People's Republic of China; ³School of Pharmacy, Nanjing Medical University, Nanjing, People's Republic of China; ⁴Department of Geriatric Neurology, Nanjing Medical University Affiliated Brain Hospital, Nanjing, People's Republic of China

Purpose: The lack of effective therapies mandates the development of new treatment strategies for vascular dementia (VaD). G protein-coupled receptor 124 (GPR124) may be a therapeutic target for angiogenesis-related diseases of CNS, including VaD. The GCPF peptide is a truncated and screened fragment of the GPR124 extracellular domain. The potential use of GCPF for VaD treatment, angiogenesis and targeting of integrin $\alpha\beta3$ are evaluated.

Methods and results: First, the in vivo results indicated that the GCPF peptide could decrease mean escape latency and increase platform crossing times in BCCAO rats. Second, the in vitro and ex vivo results indicated that the GCPF peptide was an active angiogenic peptide and could promote hCMEC/D3 cell migration and adhesion to ECM molecules. Third, in silico analyses predicted that GCPF could specifically interact with integrin $\alpha\beta3$; the ΔG of GCPF binding to the binding pocket was -16.402 KJ/mol. The molecular characteristics indicated that highly hydrophilic GCPF with a pI of 11.70 had a short half-life in mammals (~ 1 hr). Finally, the ELISA experiments indicated that low dissociation constant ($K_d = 2.412 \pm 0.455$ nM) corresponds to the high affinity of GCPF for integrin $\alpha\beta3$.

Conclusion: The data indicate that adhesion of GCPF immobilized on ECM surface to endothelial cells via integrin $\alpha\beta3$ modulates cellular functions to promote angiogenesis and improve cognitive function. This is the first report to prove that GCPF, a novel octapeptide, may be an effective strategy for VaD therapy.

Keywords: G-protein coupled receptor 124, vascular dementia, chronic cerebral hypoperfusion, angiogenesis, integrin, protein therapy

Introduction

Vascular dementia (VaD) is one of the most common causes of dementia after Alzheimer's disease (AD).¹ Because of uncertainties over disease classification and diagnostic criteria and controversy over the exact nature of the relation between cerebrovascular pathology and cognitive impairment, it is difficult to identify tractable treatment targets.²

Aging is a major risk factor of VaD. Increasing evidence reveals that angiogenesis is impaired during aging.³ Progressive impairment of cerebral angiogenesis is likely to play a central role in age-related microvascular dysfunction and development of

Correspondence: Hong Shen; Hong Xiao
Neuro-Psychiatric Institute, Nanjing
Medical University Affiliated Brain
Hospital, 264# Guangzhou Road, Nanjing
210029, People's Republic of China
Tel +86 25 8229 6334; +86 25 8229 6352
Email shenhong_nbh@njmu.edu.cn;
xhnyy123@163.com

vascular cognitive impairment (VCI).^{4,5} Thus, age-related VaD occurs due to angiogenic degeneration which induces reduced capillary density (CD) and chronic cerebral hypoperfusion (CCH) and consequently predisposes toward cognitive impairment and dementia. Support for the therapeutic corollary of the angiogenesis hypothesis comes from studies that have demonstrated that recombinant angiogenic factors (eg, vascular endothelial growth factor (VEGF)) improve motor function and memory in the local microcirculation in cerebral hypoperfusion disease.^{6–8} As such, promotion of cerebrovascular angiogenesis may be an effective strategy to treat VaD.

G protein-coupled receptor 124 (GPR124) is a membrane surface receptor, expressed in endothelial cells and pericytes in the embryo during angiogenesis; and exclusively expressed in the vascular endothelium in the brain, in angiogenic pericytes, and in epithelial tumors in adults.^{9,10} The *in vivo* studies reported that *Gpr124*-deficient mice died during the embryonic period of 15.5 days due to vascular developmental defects in the forebrain and spinal cord.¹¹ In 2017, Chang et al¹² revealed that GPR124 was a necessary factor for the integrity of BBB during pathologic injury. The striking functional tropism of GPR124 can mark this receptor as a therapeutic target for angiogenesis-related diseases of CNS.¹³

The structure of the extracellular domain of GPR124 has been determined.⁹ In 2006, Vallon et al¹⁴ found that the extracellular domain of GPR124 [termed sTEM5 (soluble TEM5)] containing a cryptic RGD motif bound to several glycosaminoglycans (GAGs) on the ECM and cell surface and mediated subsequent endothelial cell survival during angiogenesis by binding integrin $\alpha\beta3$. In 2012, Vallon et al¹⁵ reported that a 60 kDa NH₂-terminal fragment (termed N60) formed by proteolytic processing of sTEM5 with proteases could be immobilized on ECM to bind to the endothelial cell to RGD-dependent integrin $\alpha\beta3$ and subsequently modulated cellular functions such as adhesion and migration during angiogenesis. Interestingly, the adhesion of proteases-treated sTEM5 to HUVECs was increased 11-fold compared with that of the untreated protein.¹⁵ These results imply that extracellular domain fragments of GPR124 containing the RGD motif can bind to integrin $\alpha\beta3$ and subsequently induce angiogenesis and thus may be beneficial for VaD treatment.

Despite the understanding of the GPR124 structure and functions, it has not been applied for the treatment of human CNS disorders. We truncated and screened a fragment of the extracellular domain of GPR124 and named it GCPF. GCPF is an octapeptide and its full amino-acid

sequence is RGDFRWPR (Figure 1). Here, we evaluate GCPF peptide improves cognitive function in VaD via pro-angiogenesis by targeting integrin $\alpha\beta3$.

Materials And Methods

Animals

Sprague–Dawley male rats (6 to 7 weeks of age) were obtained from BK Experimental Animal Center (Shanghai, China). All animals were housed in a controlled environment (22±2 °C; 12 hrs light-dark cycle) under specific pathogen-free conditions with water and food provided *ad libitum*.

The procedures of this animal study were approved by the Animal Ethics Committee of Nanjing Medical University, performed in compliance with the same committee and following the guidelines outlined for the Care and Use of Laboratory Animals. All experiments and data analyses were performed under investigator-blinded conditions.

Cell Lines

The human cerebral microvascular endothelial cells (hCMEC/D3) were obtained from Cedarlane (CAN). The hCMEC/D3 cells (passages 28 to 33) were cultured in EBM2 medium supplemented with 5% FBS, hydrocortisone (1.4 μ M), ascorbic acid (5 μ g/mL), 1% chemically defined lipid concentrate, human bFGF (1 ng/mL), HEPES (10 μ M) and antibiotics on collagen I (150 μ g/mL)-coated flasks under 5% CO₂ at 37 °C. Every 3–4 days, cells were passaged using trypsin/EDTA (Gibco, USA) to detach the cells from the flasks.

Polypeptide Synthesis And Determination Of The Purity Of Synthesized Polypeptide

The GCPF peptide was chemically synthesized using Fmoc solid-phase peptide synthesis (SPPS). Briefly, Fmoc-Arg

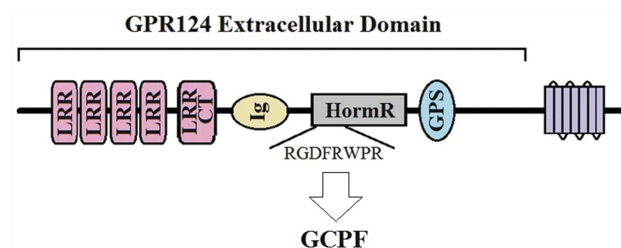


Figure 1 The GCPF peptide is a truncated and screened fragment of GPR124 extracellular domain that contains several conserved subdomains and themes: four simple leucine-rich repeat (LRR) domains, an LRR of the COOH-terminal type (LRRCT), an immunoglobulin-type domain (Ig), and a hormone-receptor domain (HormR).

(OtBu)-Wang resin used as a solid-phase material was sequentially coupled to the protected amino acids: Fmoc-Gly-OH, Fmoc-Asn(Trt)-OH, Fmoc-Phe-OH, Fmoc-Arg(tBu)-OH, Fmoc-Trp-OH, Fmoc-Pro-OH and Fmoc-Arg(tBu)-OH (Sigma, USA). The coupling reactions were performed with HOBt/DIC (1.1/1.5, v/v). After all reactions were complete, the synthesized peptide was cleaved from the resin with the lysate solution (TFA/phenol/water/thioanisole/EDT, 92:2.5:2.5:1.5:1.5, v/v/v/v). Then, the purity of synthesized polypeptide was determined using high-performance liquid chromatography (HPLC) on an Amethyst C18-H column (150 mm×4.6 mm i.d., 5 μm, Sepax, USA) with a gradient elution using buffer A (0.1% trifluoroacetic acid (TFA) in 100% water (v/v)) and buffer B (a mixture of 0.1% TFA in 80% acetonitrile and 20% water (v/v)) as the mobile phase at a flow-rate of 1.0 mL/min and UV detection at 220 nm. The gradient started from 28% and ended at 48% of buffer B. Then, the purity of the synthesized polypeptide was determined confirmed to be more than 97.5%.

Mass Spectrometry

Mass spectroscopy (MS) was used to determine the molecular weight of the synthesized GCPF. The purified sample was directly introduced into the mass spectrometer ion source. The parameters of mass spectrometer (electrospray ionization and positive ion mode) included N₂ for dry gas, flow rate 10.0 L/min, gas temperature 350°C, nebulizer pressure 40 psi and capillary pressure 4000 V. The data of mass spectrometry were processed with the MassHunter analysis software. The molecular weight was calculated with the mass-to-charge ratio (m/z).

Compute pI/Mw Tool

Analysis tool Compute pI/Mw (https://web.expasy.org/compute_pi/) was used to obtain isoelectric point (pI) and molecular weight (MW). This tool calculates the estimated pI and MW of a specified Swiss-Prot/TrEMBL entry or an amino acid sequence of interest. To use the program, protein sequence is input in a single letter code and the “click here to compute pI/Mw” button is selected. Then, theoretical pI and MW are computed.

ProtParam Tool

In vivo half-life in mammals was estimated by ProtParam (<https://web.expasy.org/protparam/>). The parameters computed by ProtParam can be deduced from a protein sequence. To use the program, a protein sequence of interest is entered using a standard single letter amino acid code and the

“compute parameters” button is selected. Then, the parameters of the estimated half-life are computed.

GRAVY Calculator Tool

The grand average of hydropathy (GRAVY) value for protein sequences was calculated with GRAVY calculator (<http://www.gravy-calculator.de/>). The GRAVY value is defined by the sum of hydropathy values of all amino acids divided by the number of residues in the sequence. Generally, a greater negative value represents higher hydrophilicity and a greater positive value represents higher hydrophobicity. To use the program, the “direct input” button is selected; a protein sequence is entered using a single letter amino acid code the “calculate” button is selected. Then, the GRAVY value is calculated.

Bilateral Common Carotid Artery Occlusion (BCCAO)

BCCAO in rats was performed as recommended.¹⁶ Briefly, after 1-week acclimatization, male adult Sprague–Dawley rats weighing 220–250 g have been fasted overnight and were anesthetized with an intraperitoneal injection of sodium pentobarbital (50 mg/kg). Then, the bilateral common carotid arteries (CCAs) were exposed and isolated from the vagus nerves. Ligations were performed from the left CCA to the right CCA. Body temperature was monitored and maintained between 36.5 and 37.5 °C with the aid of a heated pad and a blanket during the surgery. The anesthesia and surgical procedure of the sham rats were the same as that in the case of the BCCAO rats. However, when the bilateral common carotid arteries were exposed, no ligation was performed.

All rats were divided into two main groups, sham and BCCAO. On day 10, BCCAO rats were randomly assigned to 4 subgroups: BCCAO rats, BCCAO rats treated with donepezil (1.0 mg/kg once per day, i.g.) and BCCAO rats treated with GCPF at the dose of 0.5 and 1 mg/kg (3 times per day, s.c.). After surgery, treatment was administered daily from day 10 to day 23. From day 24 to day 28, the behavioral testing was assessed including the acquisition trial for 4 days and the retrieval trial on the last day (day 28). On day 28, each rat was assessed for BBB permeability and the brain was collected for histological analysis.

Morris Water Maze (MWM)

MWM is a classic test for examining spatial learning and memory in rats.¹⁷ MWM testing was conducted in a

circular pool, 180 cm across and 50 cm deep. The pool was filled to a depth of 40 cm. Pool temperature was maintained at $25 \pm 0.5^\circ\text{C}$ by the addition of warm water. Nontoxic paint was added to make the water opaque. Four points on the perimeter of the pool were used to determine 4 quadrants of the pool. A 12-cm-diameter glass platform was placed in the middle of one of the quadrants (submerged 1 cm below the water level).

The behavior tests were divided into two trials, acquisition trial and retrieval trial. The acquisition trial began by placing the rats on the platform for 20 s to allow orientation. After orientation, the rats were faced toward the wall of the pool and placed gently into the pool facing the wall at one of 4 points. The rats were allowed to search for 60 s. If the rats located the platform before 60 s, it was immediately removed from the pool. If the platform was not located after 60 s of swimming, the rats were gently guided to the platform and allowed to reorient for an additional 20 s before being removed from the pool. All rats were subjected to 4 trials per day with an intertrial interval of approximately 30 min for 4 consecutive days. From day 1 to day 4, location remained in the same position throughout all trials and days but 4 trials per day started from a different direction. The escape latency was recorded each day during acquisition trials and mean escape latency (MEL) on day 4 was used as an index of acquisition. On day 5, rats underwent the retrieval trial when the platform was removed. The rat was faced toward the wall, placed in the opposite quadrant to the platform that was previously placed and allowed to explore for 60 s. Platform crossing times were recorded for each rat. All trials were conducted at approximately the same time each day in order to minimize variability in performance due to time of day. The escape latency and the platform crossing times for each rat were recorded by two independent observers without knowledge of the experimental groups.

Histology

The collected brains were fixed in 4% paraformaldehyde (PFA) in 0.01 M PBS (pH 7.4) for 48 hrs. Fixed sub-dissected brain blocks were embedded in paraffin and serial sections (5 μm) were cut at the coronal level, mounted on glass slides and stained with haematoxylin-eosin. Neurons and vascularization in the hippocampal CA1 region were observed at 200 \times magnification. Two independent observers read the slides blindly.

Evans Blue Dye

Evans blue dye was used to study BBB permeability. Evans blue dye (4% in PBS, 4 mL/kg, Sigma-Aldrich) injections were given intravenously and the dye was allowed to circulate for 1 h. After 1 h circulation, rats were anesthetized and transcardially perfused with saline to remove the intravascular dye. Then, the brains were weighed, homogenized in 10 volumes of 50% trichloroacetic acid solution, and centrifuged. The amount of extravasated Evans blue dye was evaluated by spectrophotometry at 620 nm and quantified as A_{620}/g brain tissue.¹⁸

Cell Proliferation Assay

The 3-(4,5-dimethyl-2-thiazolyl)-2, 5-diphenyl-2-H-tetrazolium bromide (MTT, Sigma, USA) assay was used to evaluate cell proliferation. Briefly, the cells were cultured in flat-bottom 96-well plates (Costar, USA) (8×10^4 cells per well) and incubated in the medium to 90% confluence. The medium was replaced with a fresh medium-containing vehicle and GCPF (1, 10, 100, and 1000 $\mu\text{g}/\text{mL}$). hCMEC/D3 cells treated with the vehicle were used as a control. After 48 hr incubation, 20 μL MTT (5 mg/mL) was added in each well and the cells were incubated at 37°C for 4 hrs. The conversion of MTT to formazan in metabolically viable cells was spectrophotometrically measured at 570 nm with 630 nm as the reference wavelength.

Migration Assay (Scratch Wound Healing Assay)

The scratch assay was performed to demonstrate the function of GCPF in hCMEC/D3 cell migration as described with minor modifications.¹⁹ In this assay, hCMEC/D3 cells at 100% confluence in 24-well plates were wounded with a sterile pipette tip to generate a cell-free gap. Three wound locations in the culture plate were marked. The cells were incubated at 37°C in serum-free medium. To minimize the effect of cell proliferation on the wound healing assay, the medium did not contain bFGF. Then, hCMEC/D3 cells in different groups were exposed to various conditioned media containing vehicle, negative control peptide (sequence: PGDFRWPR, 10 $\mu\text{g}/\text{mL}$), VEGF (10 ng/mL) and GCPF (1, 5, 10, and 20 $\mu\text{g}/\text{mL}$). hCMEC/D3 cells treated with the vehicle were used as a control. Wound distance at the marked wound location was monitored at $\times 50$ magnifications at 0, 12 and 24 hrs. The wound distance was quantitatively evaluated using the Image-Pro Plus 6.0 software (Media Cybernetics, USA). The wound distance

reduction at the corresponding time points represented the migration distance and the migration rate (%) was calculated based on the comparison of the migration distance of experimental samples with that of the vehicle-treated control.

Tube Formation Assay

The tube formation assay is a powerful *in vitro* assay to identify inhibitors or stimulators of angiogenesis.²⁰ Briefly, 40 μ L Matrigel (BD Biosciences) was plated in each well in 96-well plates and allowed to reach the solid phase. hCMEC/D3 cells were then suspended in the treatment medium and plated on top of the Matrigel. Cells were cultured in the medium with bFGF (35 ng/mL). Cells in different groups were exposed to various conditioned media containing vehicle, negative control peptide (10 μ g/mL), VEGF (10 ng/mL), and GCPF (1, 5, 10, and 20 μ g/mL). After 12 hr incubation, the wells were imaged using an inverted phase contrast microscope (Zeiss, Axiovision). Quantification was performed blindly by counting the number of tubes.

Rat Aortic Ring Assay

The rat aortic ring assay, an *ex vivo* model, was used to identify modulators of angiogenesis.²¹ Briefly, six-week-old Sprague–Dawley rats were sacrificed and their thoracoabdominal aortas were excised. The aortas were dissected free of any fibroadipose tissue and sectioned into 0.5- to 1-mm rings. Two rat aortic rings were embedded in 35 μ L Matrigel (5 mg/mL) in each well. Basal medium-containing vehicle, negative control peptide (10 μ g/mL), VEGF (10 ng/mL) or GCPF (1, 5, 10, and 20 μ g/mL) was added. The rings were incubated in the medium for 7 days; the medium and peptides were refreshed every 2 days; after 7 days, the rings were imaged using an inverted phase contrast microscope for quantification and for an overview of the extent of microvessel sprouting. Manual vessel counting was done in a blinded setup.

Integrin $\alpha\beta 3$ Binding Assay

To confirm the binding of GCPF with integrin $\alpha\beta 3$, docking analysis was performed by the Surflex flexible molecular docking method (Sybyl-X, USA and MOE, CAN). First, the protein input file was prepared; the crystal structure of integrin $\alpha\beta 3$ (PDB: 1L5G)²² used in this study was extracted from Brookhaven Protein Data Bank (<http://www.rcsb.org/pdb>). The protein was cleaned by removing water molecules, ligands and subunits from the original integrin

$\alpha\beta 3$ PDB file. The bond orders were assigned and hydrogen atoms were added. The resulting receptor was saved as a PDB file. Second, the ligand input file was prepared; the ligand input structure of the GCPF peptide was generated and subjected to two steps of energy minimization using the steepest descent and conjugate gradient algorithm for 10,000 steps at an RMS gradient of 0.01 and 0.005, respectively. During the energy minimization process, the backbone was fixed. The GCPF structure was saved as a mol2 file. Third, molecule docking was performed using the Surflex flexible molecular docking method in order to find the preferred binding conformations of GCPF to the receptor. Docking parameters were set to the software default values. During the docking process, a maximum of 50 different conformations were considered for the ligand. The degree of binding between GCPF and integrin $\alpha\beta 3$ was evaluated by Total-Score and Chem-Score.

Determination Of The Dissociation Constant

The dissociation constant (K_d) of GCPF and integrin $\alpha\beta 3$ interaction were determined in solution by ELISA as described by Friguet et al²³ Briefly, integrin $\alpha\beta 3$ at indicated serial concentrations (0.5–32 nM) was incubated with the GCPF peptide (0.5 nM) for 4 hrs at 37°C to reach equilibrium; 150 μ g of the mixture was transferred into the 96-well polystyrene plates that were precoated with integrin $\alpha\beta 3$ antibodies (dilution 1:50, SANTA CRUZ, CA) and incubated for 1 hr at room temperature. After washing, the binding complexes were detected by ELISA. All experiments were performed in triplicates. The K_d was determined using a one-site specific binding non-linear regression (GraphPad Prism 5.0, CA).

hCMEC/D3 Cell Adhesion Assay²⁴

Ninety-six-well polystyrene plates were coated with fibronectin (FN, 10 μ g/mL) overnight at 4 °C. Wells were blocked for 1 hr with a blocking buffer. The blocking buffer was removed from the 96-well plates and the wells were washed with TBST. hCMEC/D3 cells (5×10^5 cells/well) were pre-incubated with serial dilutions of GCPF or with the vehicle for 30 mins at 37°C, added into fibronectin-coated wells and incubated at 37°C for 30 mins. After three washes with the blocking buffer to remove non-adherent cells, 100 μ L of 0.1% crystal violet solution was added to each well and incubated for 1 hr at room temperature and the absorbance was measured at 570 nm.

Statistical Analysis

All the data are expressed as the mean \pm standard deviation (SD). The paired samples *t*-test was used for group comparison between the test and control groups. The data were analyzed by using SPSS (version 13.0; SPSS Inc., Chicago, IL). For all statistical analyses, a *p* value of less than 0.05 (2-tailed) was used to test statistical significance. All reported probabilities are two-tailed.

Results

The Molecular Characteristics Of GCPF

The molecular characteristics were estimated by the Compute software. The molecular formula of GCPF, C₄₉H₇₂N₁₈O₁₁, includes 8 atomic acids and 150 atoms. The theoretical relative MW was 1089.22 Da (~1089 Da). The calculated pI was 11.70. The grand average of hydropathy value was -2.1375, which indicates that this molecule is highly hydrophilic due to the negative value. The GCPF peptide has a short half-life in mammals and the estimated half-life was only 1 hr.

After synthesis and purification, the purity of the synthesized polypeptide was confirmed to be more than 97.5% by HPLC (Figure 2A). The synthesized GCPF sample was analyzed with LC/MS in the positive mode (Figure 2B). Several ions were detected including *m/z* 273.3 ([M+4H]⁴⁺), *m/z* 364.0 ([M+3H]³⁺), *m/z* 545.4 ([M+2H]²⁺), and *m/z* 1089.5 ([M+H]⁺), which correspond to the quadruple, triple, double, and single charged

species, respectively. According to the *m/z* ion sequence, the calculated MW of the synthesized GCPF sample was 1089.17, 1088.98, 1088.79 and 1088.49 Da, respectively. The average calculated MW of the GCPF sample was 1088.86 Da (~1089 Da). The calculated value of MW was similar to the theoretical MW obtained with the Compute pI/Mw tool. The results indicate that the synthesized polypeptide has high purity and is suitable for use in *in vivo* and *in vitro* experiments.

Interaction Of GCPF With Integrin $\alpha\beta3$

We examined whether GCPF targeted integrin $\alpha\beta3$. The ligand binding to the receptor was simulated by the Surflex flexible molecular docking method. Molecular docking was assessed by Total-Score and Chem-Score.

When GCPF was prepared as the ligand input structure, NH₂-terminal residues of the ligand were changed due to GCPF carrying more positive ions in pH~ 7 physiological environments (the pI of GCPF is 11.70) considering that the charged ions do not contribute to docking. After the binding mode optimization, energy minimization and docking simulation, the structure of GCPF, the mode of integrin $\alpha\beta3$ -GCPF and the binding pocket are shown in Figure 3A. The residues of the binding pocket included A/Tyr178, A/Gln180, A/Ala213, A/Ala215, A/Asp218, A/Arg248, B/Tyr122, B/Ser123, B/Tyr166, B/Asp179, B/Met180, B/Arg214, B/Asn215, B/Ala218, B/Lys253, and B/Asn313 (Figure 3B). The binding between the ligand GCPF and the receptor integrin $\alpha\beta3$ primarily involves the side chain amino (-NH₂) hydrogen of

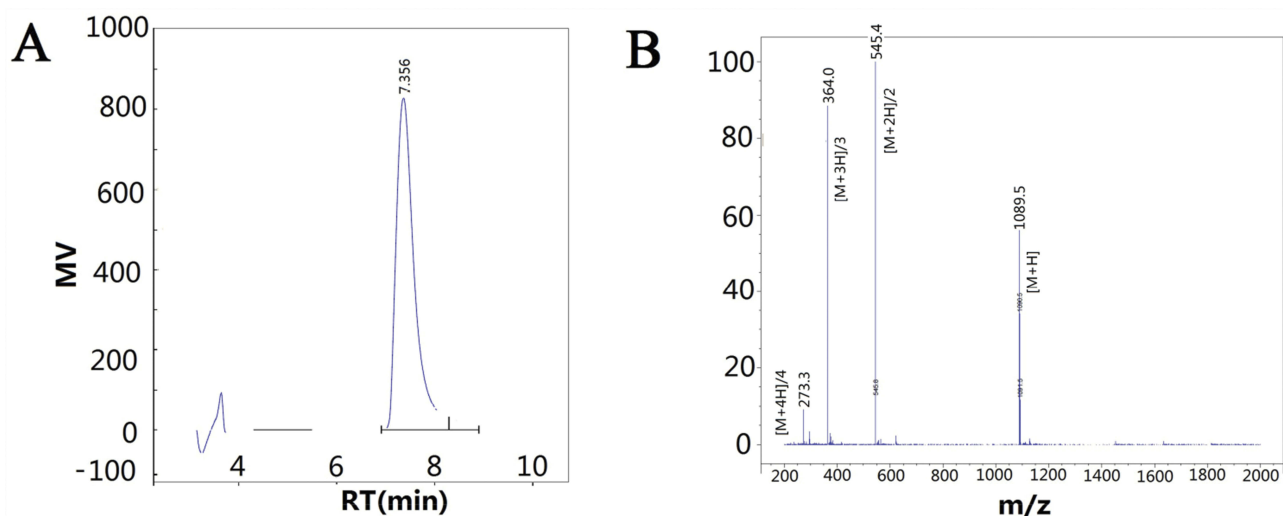


Figure 2 The data of high-performance liquid chromatography (HPLC) and mass spectra (MS).

Notes: (A) HPLC was used to determine the purity of synthesized polypeptide. Retention Time (RT) was at 7.356 min. (B) Mass spectra were obtained to determine the molecular weight of the synthesized GCPF sample. *M/z* 273.3 ([M+4H]⁴⁺), *m/z* 364.0 ([M+3H]³⁺), *m/z* 545.4 ([M+2H]²⁺), and *m/z* 1089.5 ([M+H]⁺) correspond to the quadruple, triple, double, and single charged species, respectively.

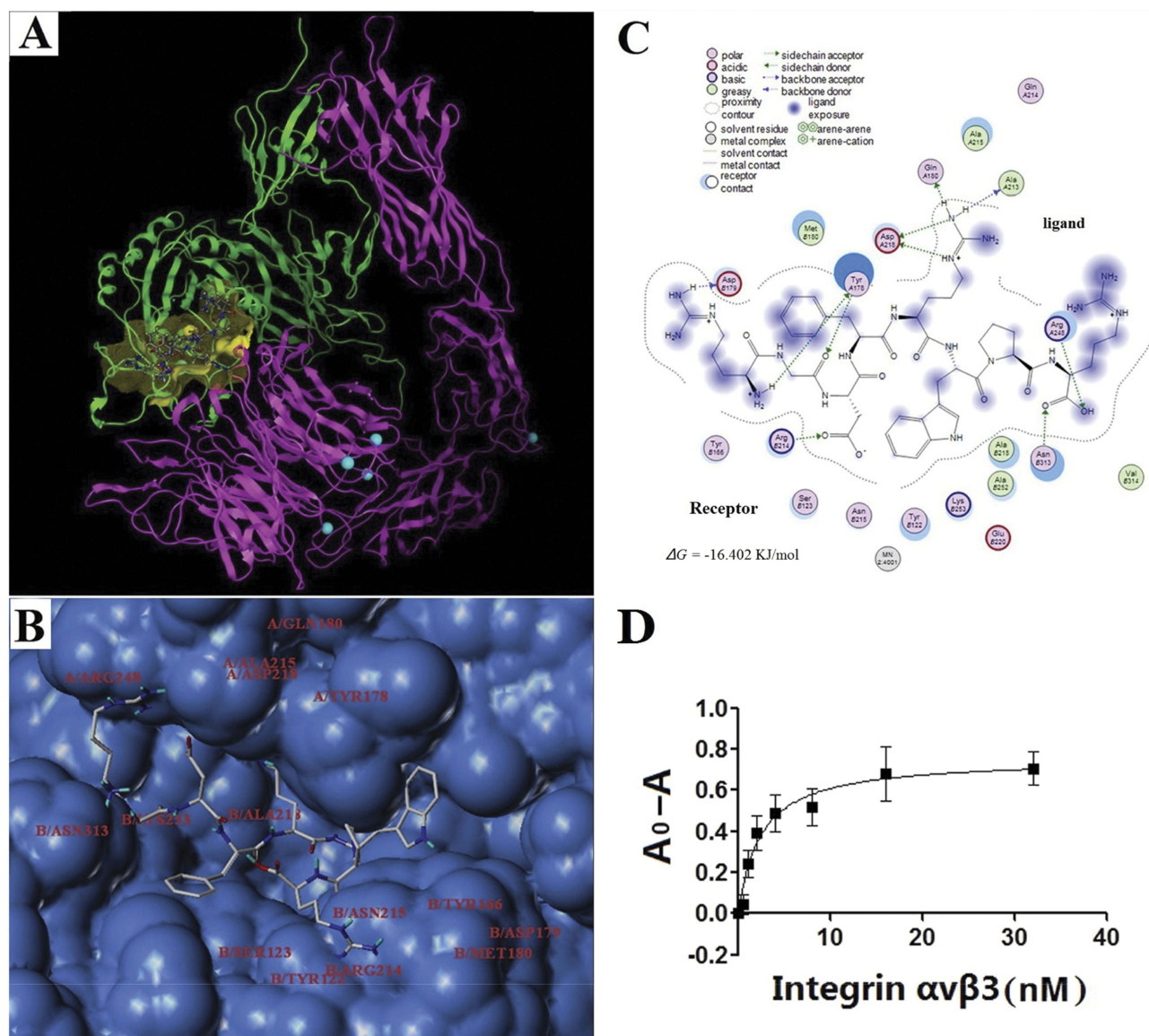


Figure 3 The GCPF peptide targets integrin $\alpha\beta 3$.

Notes: (A) Ribbon drawing of the integrin $\alpha\beta 3$ -GCPF structure simulated with molecular docking programs. In this figure, α and $\beta 3$ are shown in pink and green, respectively. The peptide is bound to the binding site (yellow). The carbon, nitrogen, and oxygen atoms of GCPF are shown in white, blue and red, respectively. The magnesium ions are shown as greenish blue balls. (B) Surface represents the GCPF-binding site. The GCPF peptide is shown as the stick model. The residues of the binding pocket in the structure of integrin $\alpha\beta 3$ are labeled. (C) The 2D image of interactions between GCPF and integrin $\alpha\beta 3$. (D) The dissociation constant of the GCPF peptide and integrin $\alpha\beta 3$ determined by ELISA experiments, where A_0 and A are the absorbance measured in the absence of the receptor and at a given concentration of the receptor, respectively. $n=3$. Mean \pm SD.

the NH_2 -terminal Arg and the residue of B/Asp179 with Arg amino ($-\text{NH}_2$) hydrogen and the side chain Gly carbonyl ($-\text{C}=\text{O}-$) oxygen contacting the A/Tyr178 residue. Apart from the RGD motif, the Asp carbonyl ($-\text{C}=\text{O}-$) oxygen combined with the B/Arg214 residue and the two side chain amino ($-\text{NH}_2$) hydrogens of the second Arg formed bonds with the A/Gln180 and A/Ala213 residues, respectively. Simultaneously, the side chain amino ($-\text{NH}_2$) nitrogen and imino ($=\text{NH}_2^+$) hydrogen of the same Arg is bound to A/Asp218. The COOH-terminal Arg hydroxyl ($-\text{OH}$) oxygen

and carbonyl ($-\text{C}=\text{O}-$) oxygen are bound to the A/Arg248 and B/Asn13 residues, respectively (Figure 3C). All binding contributed to the stability of the integrin $\alpha\beta 3$ -GCPF structure. The results of Chem-Score showed that the predicted Gibbs free energy (ΔG) of GCPF binding to the binding pocket is -16.402 KJ/mol. The calculated total score was 8.82, which predicts a high affinity of GCPF for integrin $\alpha\beta 3$.

Subsequently, ELISA experiments were performed to determine the dissociation constant of the GCPF peptide and integrin $\alpha\beta 3$. After calculation by nonlinear

regression, the results determined that the dissociation constant (Kd) of the peptide and integrin $\alpha\beta_3$ was 2.412 ± 0.455 nM ($r^2 = 0.9068$) (Figure 3D). The results indicate that GCPF has a high affinity for integrin $\alpha\beta_3$.

Efficacy Of GCPF In Vitro

(1) hCMEC/D3 cell proliferation, migration and adhesion

After 48 hr incubation, the proliferation inhibition rates of 1, 10, 100 and 1000 $\mu\text{g/mL}$ GCPF were 0.15%, 13.49%, 3.90% and 1.98%, respectively ($p > 0.05$). GCPF treatment has a small effect on hCMEC/D3 cells proliferation.

Cell migration of hCMEC/D3 cells into the acellular area was tested at various concentrations of GCPF. After 12 hrs, we observed significant stimulation of hCMEC/D3 cell migration after GCPF treatment as shown in Figure 4A. The scratched wound was almost closed in all groups at 24 hrs. Figure 4B illustrates the mean values of the migration distance at 12 and 24 hrs. The migration distances of 1, 5, 10 and 20 $\mu\text{g/mL}$ GCPF at 12 hrs were 138.4 ± 86.6 , 250.4 ± 95.7 ($t = 2.45$, $p < 0.05$), 306.9 ± 121.2 ($t = 2.97$, $p < 0.05$) and 236.9 ± 53.0 ($t = 3.10$, $p < 0.01$), respectively, more than those in the vehicle control [136.1 ± 32.6] (Figure 4B). The cell migration rates were 1.74%, 84.06%, 125.56% and 74.12% at the concentrations ranging from 1 to 20 $\mu\text{g/mL}$. The GCPF peptide at the dose of 10 $\mu\text{g/mL}$ had the best stimulatory effect.

The absorbance of all cells and the cells that were attached to fibronectin-coated wells was measured at 570 nm and the fraction of attached cells was calculated. GCPF treatment resulted in a remarkable enhancement of cell adhesion in the fibronectin-mediated tests compared to

that of the untreated cells. The adhesion rates at 1, 5, 10 and 20 $\mu\text{g/mL}$ GCPF were 54.57 ± 5.27 ($t > t(4)_{0.01}$, $p < 0.01$), 69.80 ± 9.17 ($t > t(4)_{0.01}$, $p < 0.01$), 87.44 ± 2.24 ($t > t(4)_{0.01}$, $p < 0.01$) and $67.70 \pm 8.65\%$ ($t > t(4)_{0.01}$, $p < 0.01$), respectively, and were higher than that in the vehicle control group [$32.23 \pm 5.68\%$]. (Figure 4C)

(2) The tube formation assay

hCMEC/D3 cells placed onto Matrigel formed tube-like structures that were quantified. VEGF was used as a positive control; the tube-like structures were developed from clear elongated cell bodies, which connected to form a polygon network. In the presence of GCPF, ability of hCMEC/D3 cells to form tubes was stimulated in a statistically significant manner at the concentrations ranging from 1 to 5 $\mu\text{g/mL}$ (Figure 5). The number of tubes at 5 $\mu\text{g/mL}$ GCPF at 12 hrs was 152.3 ± 1.5 ($t = 3.98$, $p < 0.05$), and was higher than that in the vehicle control group [108.0 ± 12.5]. These data indicate that GCPF has an active angiogenic effect at low concentrations.

(3) The rat aortic ring model

The effect of the GCPF peptide on angiogenic responses was assessed in the rat aortic ring model that provides a physiologically relevant in vitro model for angiogenesis characterized by the development of lumenized blood vessels with surrounding supporting cells. The results are shown in Figure 6A and B. On day 7, the GCPF peptide promoted outgrowth from the rat aortic rings in a dose-dependent manner within the dose range from 1 to 10 $\mu\text{g/mL}$; the GCPF peptide at the dose of 10 $\mu\text{g/mL}$ had the best stimulatory effect on the number of vessels [54.5 ± 17.9 ($t = 2.97$,

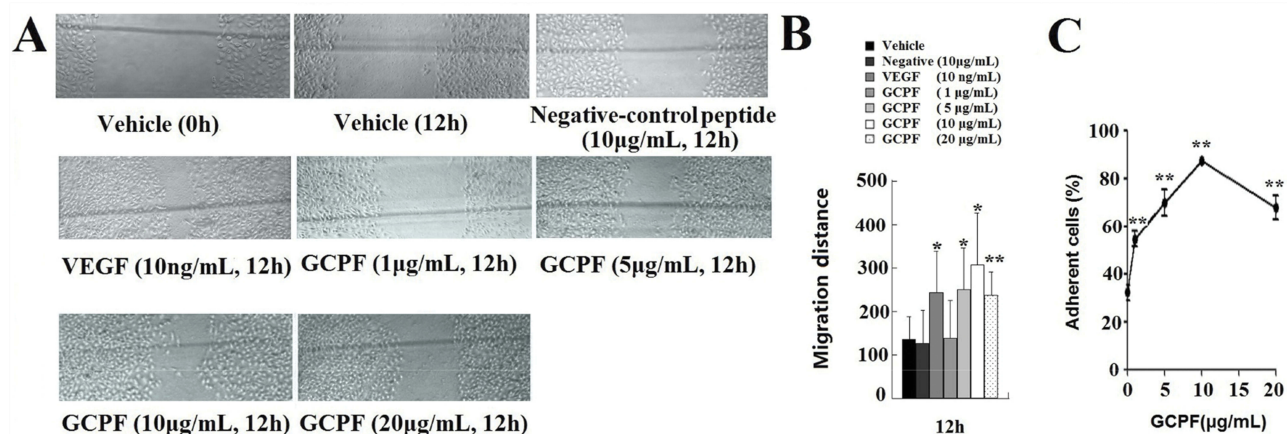


Figure 4 Effects of GCPF on hCMEC/D3 migration and adhesion.

Notes: (A) Representative images of hCMEC/D3 migration were obtained by scratch wound healing assay. The markers are shown in gray lines. (B) Histogram of the migration distance is shown. (C) The line chart of cell adhesion is shown. $n=5$. Mean \pm SD. * $P < 0.05$, ** $P < 0.01$ versus the vehicle group.

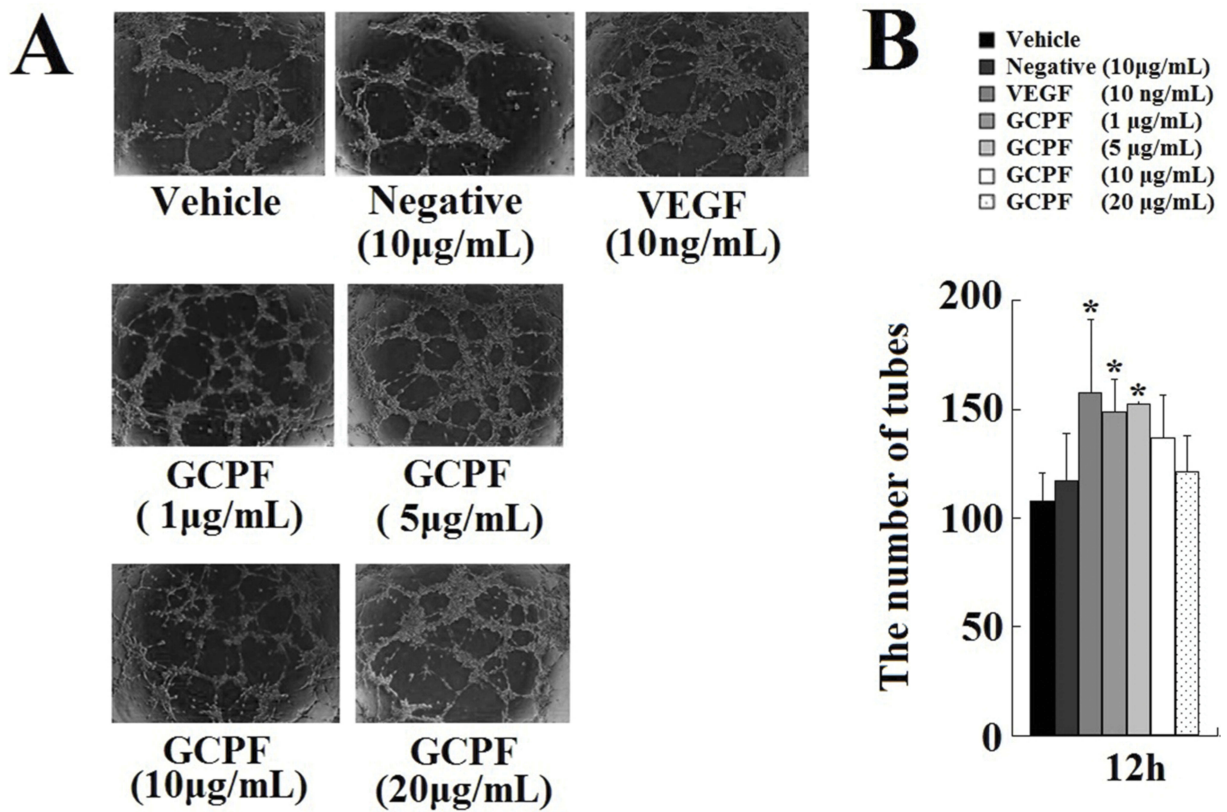


Figure 5 Effects of GCPF on the tube formation.

Notes: (A) Representative images of the tube formation. (B) Histogram of the numbers of the tubes formed. n=5. Mean ± SD. *P <0.05 versus the vehicle-treated group.

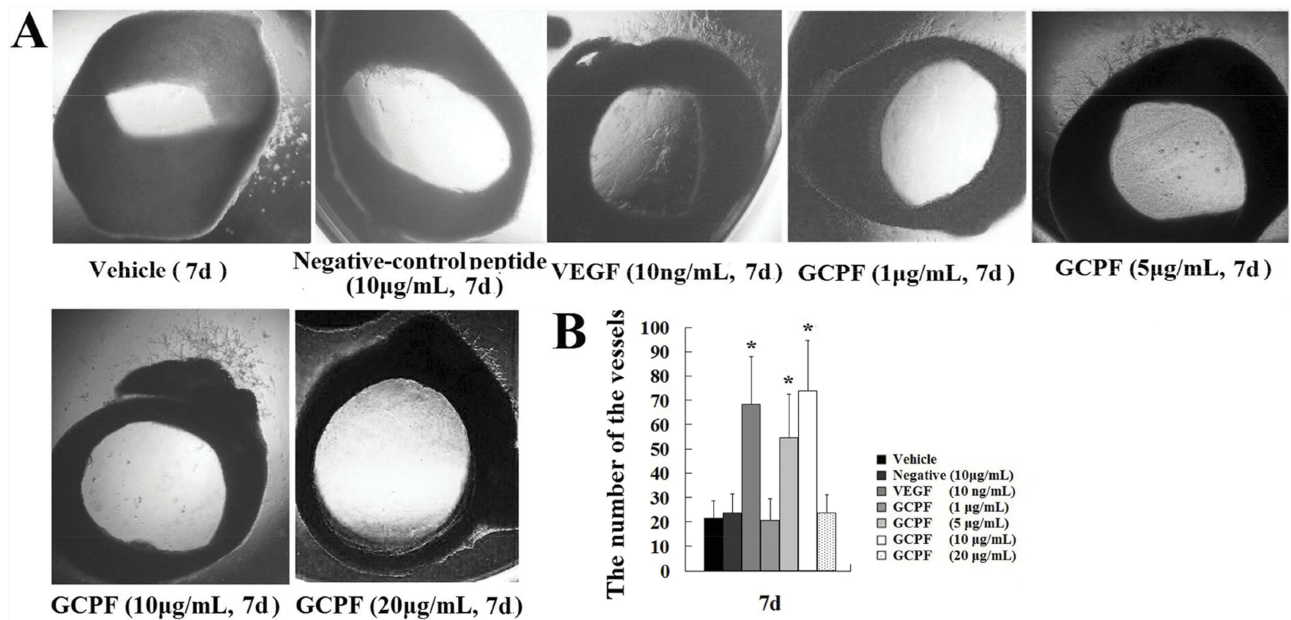


Figure 6 Effects of GCPF on the rat aortic ring.

Notes: (A) Representative images of the rat aortic ring outgrowth. (B) Histogram of the numbers of the rat aortic ring outgrowth. n=5. Mean ± SD. *P <0.05 versus the vehicle-treated group.

$p < 0.05$) and 74.0 ± 20.5 ($t = 3.62$, $p < 0.05$), respectively, versus 21.4 ± 7.2 for the vehicle control]. These *ex vivo* results revealed that GCPF is an active angiogenic stimulator.

Efficacy Of GCPF In BCCAO Rats

The MWM test was used to assess the impact of GCPF on spatial learning and memory in BCCAO rats. The results of MWM test are shown in Figure 7. On day 9, the BCCAO rats produced a significant increase in MEL compared with that in the sham rats. At the end of the acquisition trial, the administration of 0.5 and 1.0 mg/kg GCPF for 14 days resulted in a significant reduction in MEL compared with that in the untreated BCCAO rats [6.35 ± 2.11 ($t = 3.47$, $p = 0.007$), 5.05 ± 2.43 ($t = 2.85$, $p = 0.02$), respectively, versus 14.50 ± 6.78 for the untreated BCCAO rats]. Furthermore, the retrieval trial results on the last day (day 28) showed that the rats administered 0.5 and 1.0 mg/kg GCPF treatment had a significant increase in the platform crossing times compared with that in the sham rats [8.2 ± 1.8 ($t = 3.70$, $p = 0.005$), 9.4 ± 2.5 ($t = 3.83$, $p = 0.004$), respectively, versus 4.2 ± 1.5 for the untreated BCCAO rats].

To investigate a relationship between GCPF and the number of vessels or neurons in the brain, we performed a histological analysis of the hippocampal CA1 region of the brain. Representative images of haematoxylin-eosin stained CA1 region sections are presented in Figure 8. There were

fewer vessels in the hippocampal CA1 region sections in the untreated BCCAO rats [53.0 ± 8.5 versus 79.3 ± 4.2 for the sham rats ($t = 4.80$, $p < 0.01$)]. In contrast, the number of vessels was significantly increased in the hippocampal CA1 region in the GCPF (1.0 mg/kg GCPF for 14 days)-treated BCCAO rats [75.7 ± 6.7 ($t = 3.62$, $p < 0.05$) versus 53.0 ± 8.5 for the untreated BCCAO rats].

In the brain of BCCAO rats, the primary lesion occurred in the CA1 field of the hippocampus neurons including low density, disturbance and absence of the nuclei that induced a significant decrease in the number of neurons [47.3 ± 4.5 versus 93.0 ± 9.0 for the sham rats ($t = 7.86$, $p < 0.01$)]. After 0.5 and 1.0 mg/kg GCPF treatment, the number of neurons was significantly increased compared with that in the untreated BCCAO rats [64.7 ± 6.7 ($t = 3.73$, $p < 0.05$), 73.3 ± 14.4 ($t = 3.18$, $p < 0.05$), respectively, versus 47.3 ± 4.5 for untreated BCCAO rats].

To evaluate the effect on the BBB permeability, the amount of extravasated Evans blue dye was used to quantify the changes in BBB permeability. On day 28, there was no Evans blue extravasation in the untreated BCCAO rats [1.7 ± 0.8 A_{620}/g tissue, versus 1.6 ± 0.8 A_{620}/g tissue for the sham rats, $p > 0.05$, $n = 5$]. After GCPF treatment, there was no significant difference between the untreated BCCAO rats or sham rats and GCPF-treated rats in Evans blue extravasation ($p > 0.05$, $n = 5$).

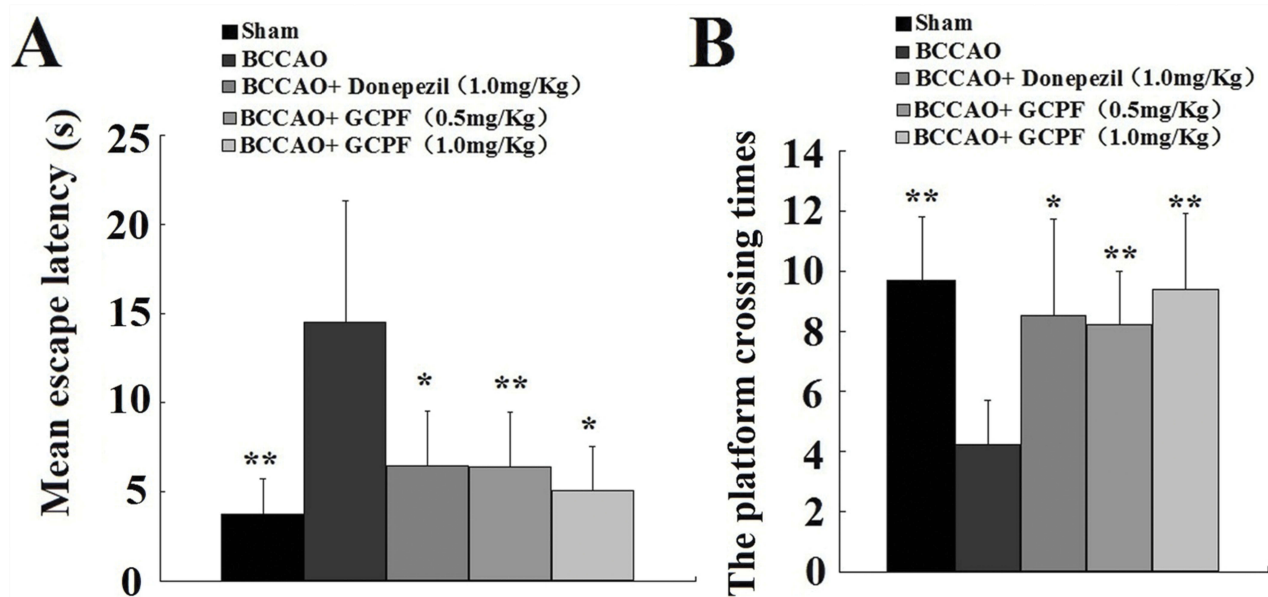


Figure 7 Effects of GCPF on learning and memory in BCCAO rats assessed with MWM.

Notes: (A) Mean escape latencies during acquisition trial were obtained from day 24 to 27. (B) The platform crossing times were assessed in the retrieval trial on day 28. $n = 10$. Mean \pm SD. * $P < 0.05$, ** $P < 0.01$ versus the untreated BCCAO rats.

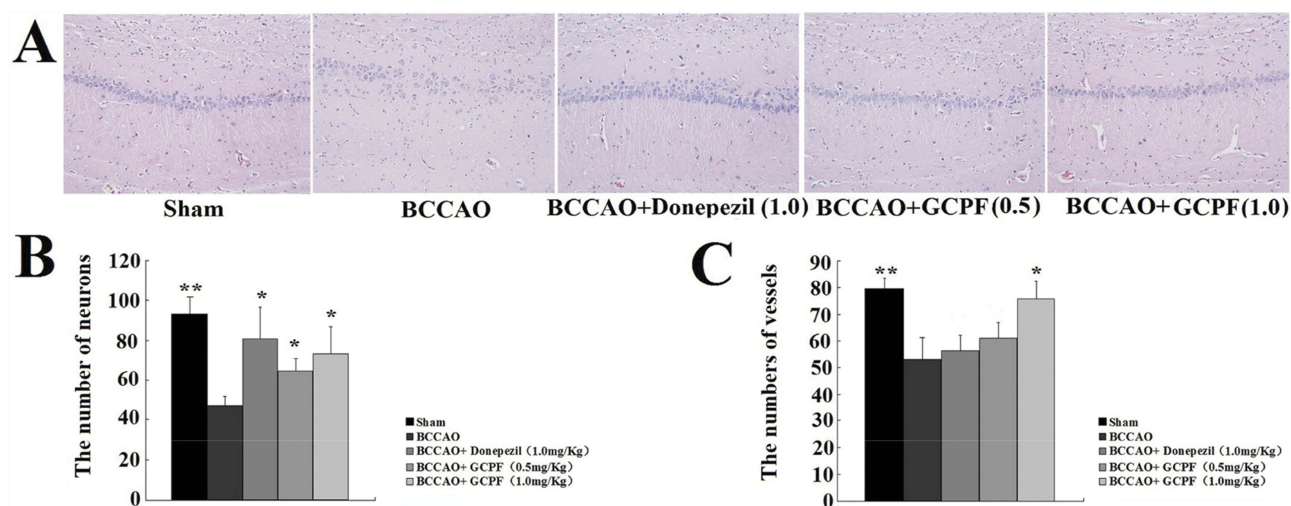


Figure 8 Effects of GCPF on the hippocampal histology in BCCAO rats.

Notes: (A) Representative H&E images of the hippocampal CA1 region sections were obtained on day 28. (B) Histogram of the number of vessels. (C) Histogram of the number of neurons. $n=5$. Mean \pm SD. * $P < 0.05$, ** $P < 0.01$ versus the untreated BCCAO rats.

Discussion

To our knowledge, we are the first to demonstrate that GCPF peptide truncated from the extracellular domain of GPR124 targets integrin $\alpha v \beta 3$, enhances in vitro and ex vivo angiogenesis and improves cognitive function in CCH-induced VaD. First, the in vivo results demonstrate that the GCPF peptide decreases MEL and increases platform crossing times in BCCAO rats. Second, the in vitro and ex vivo results indicate that the GCPF peptide is an active angiogenic promoter and enhances hCMC/D3 cell migration and adhesion to the ECM molecules. Third, in silico analyses predict that GCPF specifically interacts with integrin $\alpha v \beta 3$; the ΔG of GCPF binding to the binding pocket is -16.402 kJ/mol . The molecular characteristics suggest that highly hydrophilic GCPF with the pI of 11.70 has a short half-life in mammals (~ 1 hr). Finally, the ELISA experiments demonstrate the low dissociation constant ($K_d = 2.412 \pm 0.455 \text{ nM}$) that indicates a high affinity of GCPF for integrin $\alpha v \beta 3$.

GCPF contains the RGD motif that is present in the ECM proteins and is a major recognition sequence for integrins. The $\alpha v \beta 3$ integrin is one of the integrins that play an important role in cell adhesion and is the dominant binding receptor of the RGD motif.²⁵ The results of computer simulation indicate that the GCPF peptide targets integrin $\alpha v \beta 3$. First, GCPF is a polypeptide composed of 8 amino acids. After optimization of the binding modes and energy minimization, the GCPF sequence adopts a kinked conformation which has a very strong influence of the conformation of the RGD motif and on selectivity.

A more kinked conformation enhances binding to the integrin $\alpha v \beta 3$, while a more linear arrangement prefers binding to the integrin $\alpha IIb \beta 3$.²⁶ Second, according to the structure of integrin $\alpha v \beta 3$ -GCPF, the RGD motif of GCPF is inserted into a crevice between the αv and $\beta 3$ domains exclusively interacting with Arg, Gly and Asp side chains. Even though the RGD motif is the main contact area with the integrin, two additional Arg side chains in the GCPF sequence are involved in the interaction. The higher number of residues extensively participating in the interaction may stabilize the binding of GCPF to integrin $\alpha v \beta 3$. Third, molecular dynamics simulations of GCPF in the presence of the integrin predicted the ΔG value of -16.402 kJ/mol for GCPF binding to the binding pocket. These data indicate that GCPF binding to integrin $\alpha v \beta 3$ is spontaneous because the ΔG is negative. Finally, the K_d of the GCPF peptide and integrin $\alpha v \beta 3$ was $2.412 \pm 0.455 \text{ nM}$. Low K_d value corresponds to a high affinity of GCPF for integrin $\alpha v \beta 3$. Therefore, the RGD-containing GCPF peptide targets integrin $\alpha v \beta 3$.

Integrins are adhesion receptors on the cell surface that mediate vital bidirectional signals during morphogenesis, tissue remodeling, and repair.²⁷ Integrin $\alpha v \beta 3$, a dimeric glycoprotein, plays an important role in angiogenesis and a variety of intercellular interactions including attachment of cells to endothelium. Integrin $\alpha v \beta 3$ is a potential drug target because of its overexpression on the cells' surface, which is linked to the development and progression of various diseases, such as tumors and rheumatoid arthritis.^{28,29} Inhibitors of integrin $\alpha v \beta 3$, eg, cilengitide (the cyclic pentapeptide

cyclo(-RGDFV-)), may be used as antiangiogenics.¹⁸ Unlike cilengitide, the GCPF peptide is an active angiogenic peptide. In a series of *in vitro* and *ex vivo* angiogenic assessments, GCPF exhibited the proangiogenic bioactivities including stimulation of hCMEC/D3 cell migration and adhesion and ability to form tubes and promotion of outgrowth from the rat aortic rings. The results indicate that the GCPF peptide containing the RGD motif is a mimetic natural ligand, sTEM5, and that the GCPF peptide not only efficiently mediates cell adhesion via integrin $\alpha\beta3$ but can also elicit specific cell responses. The bioactivity of the GCPF peptide is triggered by simultaneous interaction with integrin $\alpha\beta3$ and cell adhesion to the molecules immobilized on the ECM surface (eg, fibronectin), which can explain why the GCPF peptide promotes cell adhesion.³⁰ It is of interest to know how the GCPF peptide is immobilized on the ECM surface. The results of computer analysis estimated the pI of GCPF to be 11.70. In theory, in pH~7 physiological environment, the residues of GCPF have a higher positive charge due to pI of 11.70, which results in GCPF binding to the negatively charged ECM molecules. Thus, it is evident that the hydrophilic GCPF can approach the hydrophilic ECM surface and then adhere to the ECM due to the ionic interaction of GCPF with the ECM molecules. Therefore, apart from adhesion to integrin $\alpha\beta3$, GCPF can interact with ECM and provide a favorable microenvironment to elicit cell responses. In summary, GCPF immobilized on the ECM surface during adhesion to endothelial cells via integrin $\alpha\beta3$ may modulate cellular functions, such as hCMEC/D3 cell migration, to promote angiogenesis.

Proangiogenic protein therapy uses well-defined and precisely structured proteins with well-known biological effects at predefined optimal doses of the individual protein for certain disease states.³¹ Subsequent to the proper evaluation of the molecular characteristics, structure, binding receptors and *in vitro* functions, the GCPF peptide was used to assess the impact on the *in vivo* VaD model. Several animal models mimic the VaD pathology of CCH that induces a moderate but persistent reduction in regional cerebral blood flow to compromise memory processes that contribute to the development and progression of dementia. A systematic summary suggests that chronic and not acute oligemic phase of BCCAO is the best to correspond to CCH in human aging and dementia.¹⁶ Thus, BCCAO model was used to investigate the effect of GCPF on cognitive function. The results of the present study showed that GCPF significantly reduces MEL in the BCCAO rats after 14-day administration of 0.5 and 1.0 mg/kg GCPF. The MEL

values in the acquisition trial were 6.35 ± 2.11 ($p = 0.007$) and 5.05 ± 2.43 ($p = 0.02$), respectively. Furthermore, the retrieval trial results showed that the BCCAO rats treated with two different doses of GCPF had a significant dose-dependent increase in platform crossing times [8.2 ± 1.8 ($p = 0.005$) and 9.4 ± 2.5 ($p = 0.004$), respectively] in retrieval trial. Moreover, the number of vessels and neurons in the hippocampal CA1 region of the BCCAO rats was increased by GCPF treatment according to histological analysis. The corresponding numbers in 0.5 and 1.0 mg/kg GCPF-treated BCCAO rats were 61.0 ± 6.0 ($p < 0.05$) and 75.7 ± 6.7 ($p < 0.05$) in the case of the vessels and 64.7 ± 6.7 ($p < 0.05$) and 73.3 ± 14.4 ($p < 0.05$) in the case of the neurons, respectively. These data indicate that GCPF subcutaneous injection can increase neovascularization in the hippocampus and improve spatial learning and memory in the CCH-induced VaD rat model.

Currently, several factors hinder the development of proangiogenic proteins for VaD therapy. The most important factor is the broad definition of the disease state. VaD definition recognizes the heterogeneous nature of contributions of vascular pathology to dementia and the presence of various subtypes.² A controversy in the field concerns the identification of types of vascular lesions that contribute to cognitive impairment.³² Furthermore, the broad definition of VaD means that an all-encompassing model of the disease state is not possible to achieve.³³ For example, proangiogenic therapy is beneficial for the CCH-induced VaD due to a weak effect on the BBB leakage; however, it is not suitable for brain injury caused by acute cerebral hypoperfusion, which is a sudden disruption of the blood supply to distinct brain regions leading to ischemic stroke followed by the BBB leakage. In contrast, antiangiogenic therapy via integrin $\alpha\beta3$ inhibition may ameliorate focal cerebral ischemic damage by reducing the BBB breakdown in an ischemic stroke model without motor function and memory assessments.^{34,35} The mode of delivery is another obstacle due to the short *in vivo* half-life. In our study, GCPF has *in vivo* half-life of only 1 hr and had to be administered frequently 3 times per day via a subcutaneous injection to achieve desired efficacy. Prevention of enzymatic degradation and targeting to the brain may be achieved by intranasal administration³⁶ of GCPF as an effective and noninvasive strategy for VaD therapy.

Conclusions

The present data indicate that GCPF immobilized on the ECM surface induces adhesion to endothelial cells *via*

integrin $\alpha v \beta 3$ to modulate cellular functions to promote angiogenesis and improve cognitive function. This is the first report to prove that GCPF, a novel octapeptide, may be an effective strategy for VaD therapy. However, studies of proangiogenic protein therapy for VaD are still in an early stage, and a number of clinically relevant questions remain regarding best VaD subtypes and delivery modes.

Acknowledgments

We thank China Pharmaceutical University for providing access to the Sybyl and MOE software packages. We also thank ELSEVIER author services for language editing.

Author Contributions

All authors contributed to data analysis, drafting or revising the article, gave final approval of the version to be published, and agree to be accountable for all aspects of the work.

Disclosure

The authors report no conflicts of interest in this work.

References

- Bowler JV. Modern concept of vascular cognitive impairment. *Br Med Bull.* 2007;83:291–305. doi:10.1093/bmb/ldm021
- O'Brien JT, Thomas A. Vascular dementia. *Lancet.* 2015;386(10004):1698–1706. doi:10.1016/S0140-6736(15)00463-8
- Ambrose CT. Pro-angiogenesis therapy and aging: a mini-review. *Gerontology.* 2017;63(5):393–400. doi:10.1159/000477402
- Black JE, Polinsky M, Greenough WT. Progressive failure of cerebral angiogenesis supporting neural plasticity in aging rats. *Neurobiol Aging.* 1989;10(4):353–358. doi:10.1016/0197-4580(89)90048-1
- Milner R. *Cerebral Angiogenesis: Methods and Protocols*. Clifton: Humana Press; 2014.
- Ohtaki H, Fujimoto T, Sato T, et al. Progressive expression of vascular endothelial growth factor (VEGF) and angiogenesis after chronic ischemic hypoperfusion in rat. *Acta Neurochir Suppl.* 2006;96:283–287. doi:10.1007/3-211-30714-1_61
- Thau-Zuchman O, Shohami E, Alexandrovich AG, Leker RR. Vascular endothelial growth factor increases neurogenesis after traumatic brain injury. *J Cerebral Blood Flow Metab.* 2010;30(5):1008–1016. doi:10.1038/jcbfm.2009.271
- Wang J, Fu X, Jiang C, et al. Bone marrow mononuclear cell transplantation promotes therapeutic angiogenesis via upregulation of the VEGF-VEGFR2 signaling pathway in a rat model of vascular dementia. *Behav Brain Res.* 2014;265:171–180. doi:10.1016/j.bbr.2014.02.033
- Carson-Walter EB, Watkins DN, Nanda A, Vogelstein B, Kinzler KW, St Croix B. Cell surface tumor endothelial markers are conserved in mice and humans. *Cancer Res.* 2001;61(18):6649–6655.
- Bjarnadóttir TK, Fredriksson R, Höglund PJ, Gloriam DE, Lagerström MC, Schiöth HB. The human and mouse repertoire of the adhesion family of G-protein-coupled receptors. *Genomics.* 2004;84(1):23–33. doi:10.1016/j.ygeno.2003.12.004
- Anderson KD, Pan L, Yang XM, et al. Angiogenic sprouting into neural tissue requires Gpr124, an orphan G protein-coupled receptor. *Proc Natl Acad Sci USA.* 2011;108(7):2807–2812. doi:10.1073/pnas.1019761108
- Chang J, Mancuso MR, Maier C, et al. Gpr124 is essential for blood-brain barrier integrity in central nervous system disease. *Nat Med.* 2017;23(4):450–460. doi:10.1038/nm.4309
- Kuhnert F, Mancuso MR, Shamloo A, et al. Essential regulation of CNS angiogenesis by the orphan G protein-coupled receptor GPR124. *Science.* 2010;330(6006):985–989. doi:10.1126/science.1196554
- Vallon M, Essler M. Proteolytically processed soluble tumor endothelial marker (TEM) 5 mediates endothelial cell survival during angiogenesis by linking integrin $\alpha(v) \beta 3$ to glycosaminoglycans. *J Biol Chem.* 2006;281(45):34179–34188. doi:10.1074/jbc.M605291200
- Vallon M, Aubele P, Janssen KP, Essler M. Thrombin-induced shedding of tumour endothelial marker 5 and exposure of its RGD motif are regulated by cell-surface protein disulfide-isomerase. *Biochem J.* 2012;441(3):937–944. doi:10.1042/BJ20111682
- Farkas E, Luiten PG, Bari F. Permanent, bilateral common carotid artery occlusion in the rat: a model for chronic cerebral hypoperfusion-related neurodegenerative diseases. *Brain Res Rev.* 2007;54(1):162–180. doi:10.1016/j.brainresrev.2007.01.003
- Morris RGM, Garrud P, Rawlins JN, O'Keefe J. Place navigation impaired in rats with hippocampal lesions. *Nature.* 1982;297(5868):681–683. doi:10.1038/297681a0
- Liu R, Wen Y, Perez E, et al. 17 β -Estradiol attenuates blood-brain barrier disruption induced by cerebral ischemia-reperfusion injury in female rats. *Brain Res.* 2005;1060(1–2):55–61. doi:10.1016/j.brainres.2005.08.048
- Liang CC, Park AY, Guan JL. In vitro scratch assay: a convenient and inexpensive method for analysis of cell migration in vitro. *Nat Protoc.* 2007;2(2):329–333. doi:10.1038/nprot.2007.30
- Arnaoutova I, Kleinman HK. In vitro angiogenesis: endothelial cell tube formation on gelled basement membrane extract. *Nat Protoc.* 2010;5(4):628–635. doi:10.1038/nprot.2010.6
- Aplin AC, Nicosia RF. The rat aortic ring model of angiogenesis. *Methods Mol Biol.* 2015;1214:255–264. doi:10.1007/978-1-4939-1462-3_16
- Xiong JP, Stehle T, Zhang R, et al. Crystal structure of the extracellular segment of integrin $\alpha v \beta 3$ in complex with an Arg-Gly-Asp ligand. *Science.* 2002;296(5565):151–155. doi:10.1126/science.1069040
- Friguet B, Chaffotte AF, Djavadi-Ohanian L, Goldberg ME. Measurements of the true affinity constant in solution of antigen-antibody complexes by enzyme-linked immunosorbent assay. *J Immunol Methods.* 1985;77(2):305–319. doi:10.1016/0022-1759(85)90044-4
- Humphries MJ. Cell-substrate adhesion assays. *Curr Protoc Cell Biol.* 1998;9.1.1–9.1.11. doi:10.1002/0471143030.cb0901s00
- Pierschbacher MD, Ruoslahti E. Cell attachment activity of fibronectin can be duplicated by small synthetic fragments of the molecule. *Nature.* 1984;309(5963):30–33. doi:10.1038/309030a0
- Haubner R, Gratiar R, Diefenbach B, Goodman SL, Jonczyk A, Kessler H. Structural and functional aspects of RGD-containing cyclic pentapeptides as highly potent and selective integrin $\alpha v \beta 3$ antagonists. *J Am Chem Soc.* 1996;118(32):7461–7472. doi:10.1021/ja9603721
- Giancotti FG, Ruoslahti E. Integrin signaling. *Science.* 1999;285(5430):1028–1032. doi:10.1126/science.285.5430.1028
- Santulli G, Basilicata MF, De Simone M, et al. Evaluation of the anti-angiogenic properties of the new selective $\alpha v \beta 3$ integrin antagonist RGDchiHCit. *J Transl Med.* 2011;9(1):7. doi:10.1186/1479-5876-9-7
- Shen H, Han HB, Hu JL, et al. PEGylated HM-3 presents anti-rheumatic bioactivity by inhibiting angiogenesis and inflammation. *J Mater Chem B.* 2014;2(7):800–813. doi:10.1039/C3TB21100B
- Hersel U, Dahmen C, Kessler H. RGD modified polymers: biomaterials for stimulated cell adhesion and beyond. *Biomaterials.* 2003;24(24):4385–4415. doi:10.1016/s0142-9612(03)00343-0
- Santulli G. *Angiogenesis Insights from a Systematic Overview*. New York: Nova Science; 2013.
- Gorelick PB, Scuteri A, Black SE, et al. Vascular contributions to cognitive impairment and dementia: a statement for healthcare professionals from the american heart association/american stroke association. *Stroke.* 2011;42(9):2672–2713. doi:10.1161/STR.0b013e3182299496

33. Helman AM, Murphy MP. Vascular cognitive impairment: modeling a critical neurologic disease in vitro and in vivo. *Biochim Biophys Acta*. 2016;1862(5):975–982. doi:10.1016/j.bbdis.2015.12.009
34. Shimamura N, Matchett G, Solaroglu I, Tsubokawa T, Ohkuma H, Zhang J. Inhibition of integrin α v β 3 reduces blood-brain barrier breakdown in focal ischemia in rats. *J Neurosci Res*. 2006;84(8):1837–1847. doi:10.1002/jnr.21073
35. Shimamura N, Matchett G, Yatsushige H, Calvert JW, Ohkuma H, Zhang J. Inhibition of integrin α v β 3 ameliorates focal cerebral ischemic damage in the rat middle cerebral artery occlusion model. *Stroke*. 2006;37(7):1902–1909. doi:10.1161/01.STR.0000226991.27540.f2
36. Li R, Huang Y, Chen L, et al. Targeted delivery of intranasally administered nanoparticles-mediated neuroprotective peptide NR2B9c to brain and neuron for treatment of ischemic stroke. *Nanomedicine*. 2019;18:380–390. doi:10.1016/j.nano.2018.10.013

Drug Design, Development and Therapy

Dovepress

Publish your work in this journal

Drug Design, Development and Therapy is an international, peer-reviewed open-access journal that spans the spectrum of drug design and development through to clinical applications. Clinical outcomes, patient safety, and programs for the development and effective, safe, and sustained use of medicines are a feature of the journal, which has also

been accepted for indexing on PubMed Central. The manuscript management system is completely online and includes a very quick and fair peer-review system, which is all easy to use. Visit <http://www.dovepress.com/testimonials.php> to read real quotes from published authors.

Submit your manuscript here: <https://www.dovepress.com/drug-design-development-and-therapy-journal>